

# EXPERIMENTAL HF RADAR FOR SUB-SURFACE SENSING\*

E. Douglas Lynch

Russell D. Brown, David D. Mokry, James M. VanDamme, Michael C. Wicks  
Air Force Research Laboratory Radar Signal Processing Branch (SNRT)  
26 Electronic Parkway, Rome, NY 13441-4514  
dougl@rl.af.mil

Jeff A. Brandstadt, Alan D. George, Mike A. Krumme  
Black River Systems Company, 5727 Walker Rd., Utica, NY 13502  
brandsta@brsc.com

## ABSTRACT

This paper describes our experimental approach for high frequency (HF) radar sub-surface profiling, and the results obtained from signal and data processing for deep tunnel detection. Ongoing experiments employ a bistatic radar system designed to detect buried objects located in the near-field of the sensor. Data analysis requires the use of Synthetic Aperture Radar (SAR) processing to focus the image. The experiments and initial results are based upon the use of surface contact antennas as part of a larger effort with an ultimate goal of collecting data via airborne sensors. One immediate goal of this in-house effort is to determine the resolution achievable at depths commensurate with buried structures of strategic importance. This paper also examines the trade-off between frequency and propagation in an attempt to effect the best resolution possible.

Key words: underground structures, below ground imaging, ground penetrating radar, HF radar

## INTRODUCTION

The proliferation of underground structures for military command and control posts as well as the manufacture and storage of weapons of mass destruction has increased the need for remote sensing technologies providing for the detection and identification of such facilities. One promising technology contributing to this capability, is high frequency (HF) radar. Remote sensing via HF radar could provide the depth of penetration and resolution required to detect and clearly identify such facilities, while operating at safe distances. This paper presents our approach to data collection in the first phase of our experimental program, as well as initial results

from signal processing and data analysis. This includes pulse compression, equalization, near field focusing and compensation for variation in dielectric constant.

## DESCRIPTION OF EXPERIMENT

To produce a three dimensional image of an underground drift or tunnel, an experiment was conducted to collect data over a two dimensional grid on the surface (see Figure 1). Near field focusing was performed digitally to combine the

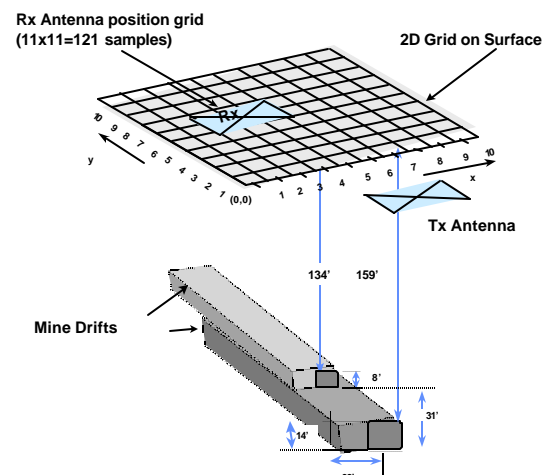


Figure 1. 2-D Grid Data Collection Geometry

data collected at each grid point and form the 3D image. The data was collected in a bistatic configuration over a grid pattern of 100ft by 100ft. Data collection points were centered at intervals of 10ft throughout the grid, with measurements performed sequentially. A single transmit antenna was located 60ft from the center point of the data collection grid. The data was collected over two drifts (horizontal mine shafts) at a depth of 159ft (48.5 meters) and 134ft (40.8 meters).

\* Presented at the 7<sup>th</sup> International Conference on Ground-Penetrating Radar, 27-30 May, 1998, Lawrence, KS.

The mine drifts are part of an extensive zinc mining operation in Upstate New York. AFRL/Rome Research Site has a Cooperative Agreement with the management of the Zinc Corporation of America (ZCA) to use their mine on a non-interfering basis. The drifts were cut through solid rock with a diameter of between 8 and 12 ft. The ceiling for about +/- 45 degrees was covered with a open wire mesh similar to fence material. The mesh was held in place with steel rods and large washers driven up into the rock ceiling. The mesh prevents debris from falling on equipment and personnel. Conduit containing power and ventilation was located near the edge of the mesh on one side and was continuous throughout the mine. The interior of the mine was very damp with wet walls and floor. The surface above the mine drifts where the data was collected was flat, hard packed crushed rock. No organic matter covered the surface.

Data was collected using ground contact antennas. The radar required a set of antennas that were wideband, directive, planar, efficient, and easily fabricated. These conflicting requirements quickly narrowed down the available choices to spiral and bowtie designs. A spiral antenna is ideal from a size vs. bandwidth standpoint, but the impedance match was highly dependent on the accuracy of the spacing and would be difficult to fabricate accurately. A bowtie antenna was better from the fabrication aspect, the resulting linear polarization was not a problem. Our antennas use a copper foil tape glued to large (10ft by 30ft) tarps, so that deployment consists of merely stretching the tarps out on the ground. A balun is used at the center of the antenna to match impedance to the 50 ohm coaxial feed cable. The antenna is about a quarter wavelength at the lowest frequency of interest, resulting in a combination of bowtie (frequency independent) and dipole operation. This results in a reasonably efficient, wideband antenna that can be easily deployed. Matching (S11) tests verified the performance of the antennas, range tests (over a dielectric half-space) are planned for the future. Data presented in this paper is based on bistatic operation with two bowtie antennas. To reduce the size of the first generation bowtie antennas, the design was revisited. On receive, the signal was not limited by receiver noise, so a lower gain antenna could also be tolerated. This made feasible an active antenna consisting of an electrically short dipole

with a matching amplifier. The amplifier matches the high antenna impedance to the receiver cable. The amplifier has differential inputs to provide a balun function, and amplifier power is fed through the coaxial cable from the receiver. No tuning is used, so the response is flat over the band of interest. Range tests with the small receive antenna are planned for the future.

The waveform used was frequency modulated – continuous wave (FM-CW) because it provides precise timing and control as well as a low peak power and high dynamic range. A 60 megahertz (MHz) bandwidth, down-ramp, LFM (Linear Frequency Modulation) waveform operating over the frequency range from 66 MHz to 6MHz was employed in our data collection experiments. This frequency range was used because of the trade-off between resolution and penetration depth. Our goal was to achieve a resolution on the order of 3ft. The transmit power into the antenna was 10 watts, provided by a solid state amplifier which was placed as close as possible to the antenna feed to minimize cable reflection. A 2 millisecond (msec) FM-CW ramp rate was employed. The receive waveform was amplified, filtered and mixed with a delayed replica of the transmit waveform to produce a baseband signal which was digitized using an IOtech data acquisition board with a 16 bit, 100 kilohertz (kHz) analog-to-digital converter (see Figure 2).

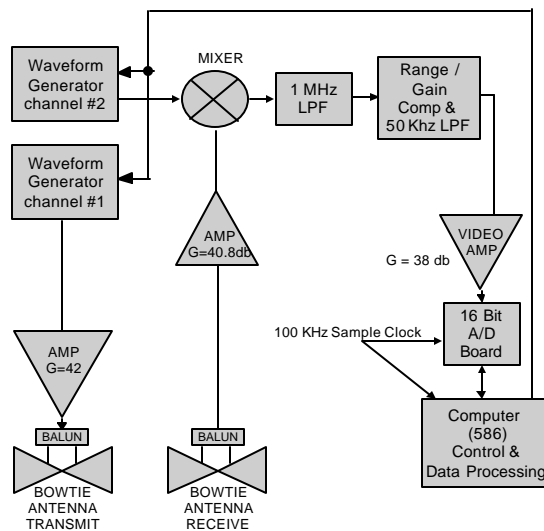


Figure 2. System Block Diagram

This sample rate provides 200 sample points per pulse and during our testing we collected 900 pulses per antenna location (see Figure 3). With a slope-chirp of 30MHz/msec, which is equivalent to 240Hz/ft (in soil with a dielectric constant of 16), our sensor provides 208ft unambiguous range for deep penetration. Commercial laboratory equipment was used for the waveform generation during this experiment. The A/D data collection board was an IOtech unit operating in a 586 based PC.

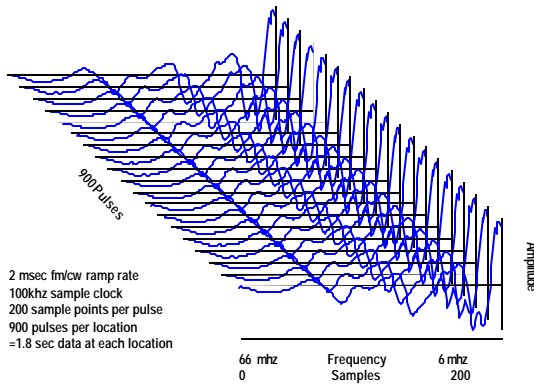


Figure 3. Data Collection Routine

## SIGNAL AND DATA PROCESSING

Since direct digital synthesis of a LFM waveform is accomplished via a LeCroy LW400 Series Arbitrary Waveform Generator (AWG), considerable flexibility is offered in the signal and data processing chain. The interpulse period is randomized on transmit (staggered) to provide for the suppression of coherent narrow band interference. Preprocessing is performed in order to reduce the effects of interference anomalies, and provide integration gain against thermal noise. This preprocessing includes pulse destagger, followed by statistical selection of the “best data” for SAR processing. This results in 123 data vectors (of length 200) which are averaged to produce a final data set. Next, normalization of amplitude versus frequency as a function of bistatic range (depth) is accomplished. High pass filtering is performed to reject strong returns from surface scatterers. Next, conversion to the complex data domain via the Hilbert Transform facilitates near field beamforming since a phase shift of the data can be accomplished by complex multiplication.

Finally, autoregressive modeling (of order 32) and linear prediction provides data extrapolation from 200 to 512 data points. This pre-processing is described in detail in Figure 4.

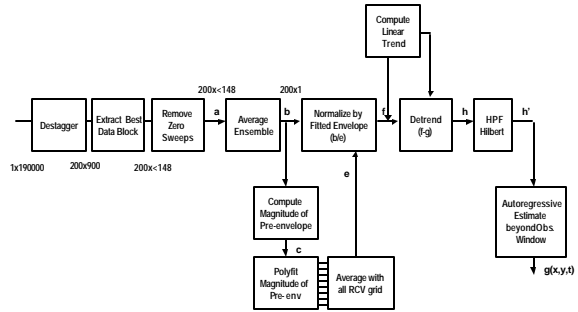


Figure 4. GPR Signal Pre-Processing

The graphical results from non-focused processing using measured data are shown in Figure 5. The figure shows plots of magnitude of the raw data at each pixel. At this stage the data has been destaggered, and digital signal processing using weighted FFT's has been accomplished.

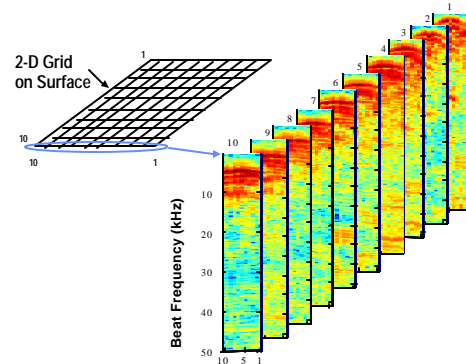


Figure 5. Pre-Processed Cuts Perpendicular to Drift

In Figure 6, a technique for near-field SAR focusing is described in detail. Due to the homogeneous nature of the earth at the ZCA Gouverneur NY test site used in this data collection, near-field SAR focusing based upon average values of permittivity resulted in excellent images. A relative path length difference to each receive antenna (location) in the plane of the SAR receive antenna is required in order to calculate phase shifts (compensation)

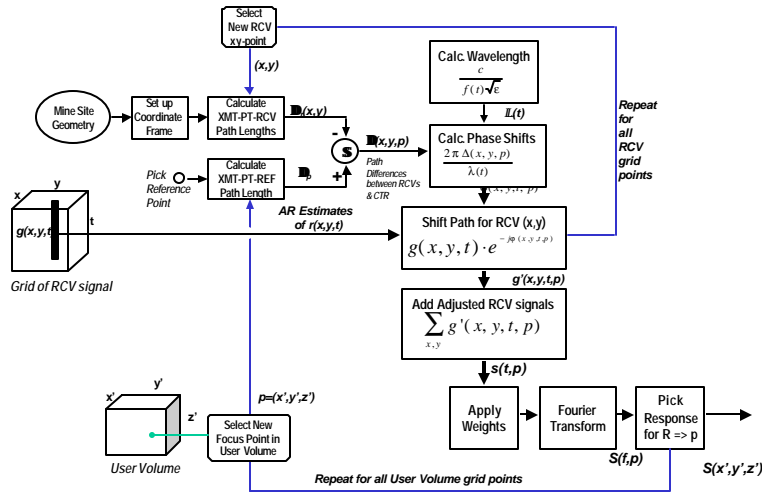


Figure 6. SAR Focusing

for beamforming. Once averaged data from each antenna location is compensated for phase versus frequency (accomplished via a complex array multiply) for near field focusing, only a final vector summation is required to integrate the data in the frequency domain. A Blackman window is applied for sidelobe suppression prior to pulse compression, which is implemented via a Fourier transform into the time (range) domain. The resulting test statistic is plotted (gray scale) as a function of range (constant depth) and cross range (horizontal displacement) to produce a SAR image.

## RESULTS

Figure 7 shows a three dimensional SAR image in gray scale. The mine drifts at 134ft and 159ft are

easily identified. With a system resolution of approximately 5ft., the two drifts are clearly observed. The additional strong returns at the shallower depth may be due to known but unmapped abandoned drifts.

## CONCLUSIONS

Our experimental program for deep penetrating radar technology development has resulted in a database for algorithm development and concept demonstration. Initial results from a data collection campaign in Gouverneur, NY indicates that our HF surface contact radar operating over the 66 to 6 MHz band provides discontinuity feature detection to a depth of 159ft (48.5m) with 5ft resolution. This technology offers the potential for remote sensing of manmade

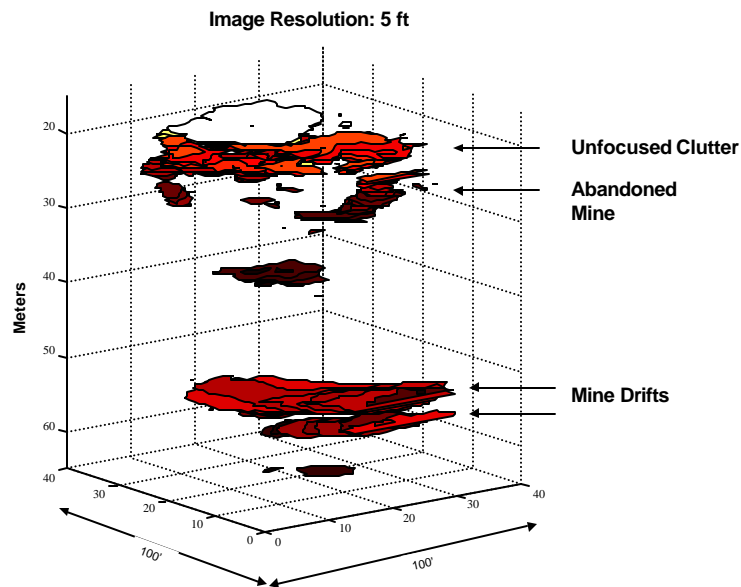


Figure 7. Focused SAR Image

structures to depths of several hundred feet. A LFM waveform generated via direct digital synthesis offers precise waveform generation and long coherent dwells for sensitive, high-resolution data processing.

#### **FUTURE EFFORTS**

Future plans for this effort include both characterizations of components and improvements to the system. The electrically small dipole antenna will be measured for directive gain (into the ground), as a function of the permittivity of the ground. Achievable resolution of the SAR image processing will be quantified. All image formation to date has been performed with both transmit and receive antennas in ground contact. Use of a small dipole antenna will permit data collection and image formation with the antenna located off the ground surface, which is the next step required before airborne system development. Also, a dipole antenna will permit data collection from moving platforms as well as over larger physical areas. Image formation processing improvements are also planned, including auto focusing to compensate for varying ground permittivity, and additional rejection of surface clutter.

The Authors wish to thank the Zinc Corporation of America for the use of their facilities for these experiments and Mr. Don Baker in particular for his expertise and cooperation in site selection and support.

#### **REFERENCES**

- Daniels, D.J., Surface Penetrating Radar, The Institute of Electrical Engineers, 1996.
- Marple, S.C., Digital Spectral Analysis with Applications, Prentice-Hall Inc., Englewood Cliffs, NJ, Chpt 8, 1987.
- Miller, R.M., Fourth Tunnel Detection Symposium on Subsurface Exploration Technology, DTIC Rpt ADA 276-372, 1993.
- Skolnik, M.I., Introduction to Radar Systems, 2nd Edition, McGraw-Hill, 1970.

#### **ACKNOWLEDGMENTS**